AIP | Journal of Applied Physics

Graphene folding on flat substrates

Xiaoming Chen, Liuyang Zhang, Yadong Zhao, Xianqiao Wang, and Changhong Ke

Citation: Journal of Applied Physics **116**, 164301 (2014); doi: 10.1063/1.4898760
View online: http://dx.doi.org/10.1063/1.4898760
View Table of Contents: http://scitation.aip.org/content/aip/journal/jap/116/16?ver=pdfcov
Published by the AIP Publishing

Graphene folding on flat substrates

Xiaoming Chen,[1] Liuyang Zhang,[2] Yadong Zhao,[1] Xianqiao Wang,[2] and Changhong Ke[1,a)]
[1]*Department of Mechanical Engineering, State University of New York at Binghamton, Binghamton, New York 13902, USA*
[2]*College of Engineering, University of Georgia, Athens, Georgia 30602, USA*

(Received 31 July 2014; accepted 9 October 2014; published online 23 October 2014)

We present a combined experimental-theoretical study of graphene folding on flat substrates. The structure and deformation of the folded graphene sheet are experimentally characterized by atomic force microscopy. The local graphene folding behaviors are interpreted based on nonlinear continuum mechanics modeling and molecular dynamics simulations. Our study on self-folding of a tri-layer graphene sheet reports a bending stiffness of about 6.57 eV, which is about four times the reported values for monolayer graphene. Our results reveal that an intriguing free sliding phenomenon occurs at the interlayer van der Waals interfaces during the graphene folding process. This work demonstrates that it is a plausible venue to quantify the bending stiffness of graphene based on its self-folding conformation on flat substrates. The findings reported in this work are useful to a better understanding of the mechanical properties of graphene and in the pursuit of its applications.
 [http://dx.doi.org/10.1063/1.4898760]

I. INTRODUCTION

Graphene is a type of emerging two-dimensional nanostructure with extraordinary mechanical and electrical properties,[1,2] and has been investigated for a number of applications, such as nanoelectronics, sensors, and composites.[3–5] Due to its ultra-thin characteristics, graphene can easily fold under external stimuli such as mechanical forces.[6] Self-folding and self-collapse behaviors of graphene have also been reported.[7–9] Understanding the mechanical deformation in folded graphene is of importance to explore its electronics application because the local deformation of graphene has a substantial influence on its electrical properties.[10,11] Graphene folding is also an essential process in manufacturing graphene origami, a programmable nanoscale building block.[9,12–14] From a structural perspective, the conformation of a self-folded graphene sheet results from a competition between its bending rigidity and adhesion interactions. Because graphene possesses a high Young's modulus, there is little or no in-plane stretching deformation in folded graphene. Therefore, it is a possible venue to quantify the pure bending stiffness of graphene through measuring its folding conformation. It is noted that the bending stiffness of graphene was previously investigated using electrostatic bending methods,[15] in which doubly clamped graphene sheets were pulled down by electrostatic forces. The bending stiffness of graphene obtained by using this method is inevitably influenced by its in-plane stretching effect, which could dwarf its bending effect even under a modest deflection.

The possible approach of quantifying the bending stiffness of graphene based on its self-folding behavior requires a complete understanding of the graphene self-folding mechanism, in particular, the role of the graphene bending stiffness in its folding conformation. As a sophisticated nanoscale physical phenomenon, graphene folding behaviors have been previously investigated using a variety of experimental and theoretical techniques. High resolution atomic force microscopy (AFM)[11] and transmission electron microscopy (TEM)[7] have been employed in the study of graphene folding on flat substrates or in suspended conditions. These high resolution imaging techniques enable measurements of the structural and folding configurations of graphene with nm or sub-nm spatial solutions. The self-folding behavior of mono- and multi-layer graphene sheets have been also investigated using both continuum mechanics (CM) and molecular dynamics (MD) simulation techniques.[8,16] These theoretical studies provide useful insights on their local folding behaviors, some of which may not be readily obtainable in experimental measurements (e.g., graphene local folding curvatures). Therefore, combined experimental and theoretical investigations are essential to a complete elucidation of the nanoscale graphene self-folding mechanism. However, such combined experimental-theoretical studies of graphene folding behaviors remain sparse in the literature. In this paper, we present a study of graphene self-folding behaviors by using AFM in conjunction with nonlinear CM modeling and MD simulations. The study focuses on the local folding behavior of few-layer graphene sheets and their bending rigidities, and provides insights into the interlayer interaction during the graphene folding process. To the best of our knowledge, this work is the *first* attempt of quantifying the bending rigidity of graphene based on experimental measurements and theoretical modeling and simulations of its self-folding conformations.

II. RESULTS AND DISCUSSION

A. Atomic force microscopy characterization of self-folded graphene

Graphene flakes employed in this study were obtained through mechanically exfoliating highly ordered pyrolytic graphite (HOPG) films,[2] and were subsequently transferred

a)Author to whom correspondence should be addressed. Electronic mail: cke@binghamton.edu

to a flat silicon oxide (SiO_2) substrate. Some of the graphene sheets were found to be in folded or partially folded conformations. Figure 1(a) shows an AFM image of a partially folded graphene sheet that is of particular interest. The AFM measurements were performed inside an XE-70 AFM from Park Systems that operates at a tapping mode with a silicon AFM tip (Vista Probe, nominal tip radius ~10 nm). It can be clearly seen from the AFM topography image that a portion of the graphene sheet (~100 nm in width) was torn and flipped on top of the flat segment on the substrate. The white dashed lines in Figure 1(a) mark the presumably original edge positions of the flipped graphene segment. The tearing of the graphene sheet occurred along almost a straight line. Therefore, the lower edge of the flipped graphene segment is most likely along either the armchair or zigzag orientation because these are the two preferred orientations in the crack propagation in graphene.[17]

To reveal the structure (e.g., the thickness and the number of layers) and the local folding deformation, we plot the respective AFM line profiles of the folded and the non-folded graphene segments along the blue and the red dashed lines marked in Figure 1(a), respectively. Figure 1(b) shows the AFM line profile of the folded graphene segment, which displays a couple of steps and one hump that corresponds to the folding edge. The lower step, whose height is measured to be about 1.56 nm, represents the height of the flat non-folded graphene segment on the substrate. This is also confirmed by the line profile of the non-folded segment shown in Figure 1(c). The upper step height shown in Figure 1(b) represents the thickness of the flipped graphene segment and is measured to be about 1.07 nm above the bottom segment. It is noted that the measured height of a graphene sheet on a flat substrate is reportedly higher than its actual thickness. For instance, the theoretical thickness of monolayer graphene is about 0.34 nm. However, its AFM-measured height is reported to be within the range of 0.5–1.0 nm.[18,19] Similar phenomena were also reported on multilayer graphene.[20] The discrepancy between the actual thickness of graphene

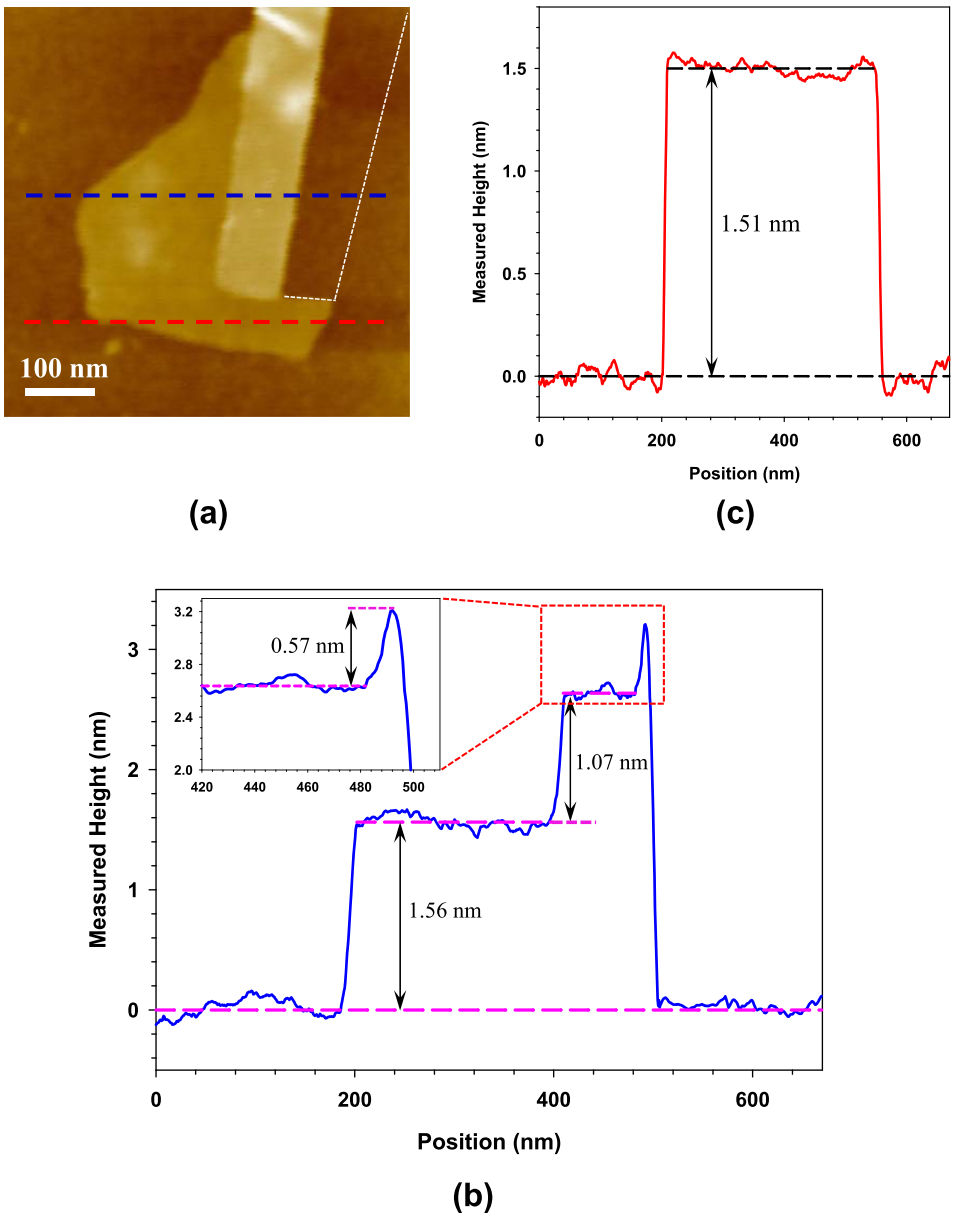

FIG. 1. (a) AFM image of one partially folded graphene sheet on a flat silicon oxide substrate. The white dashed lines mark the presumably original edge positions of the flipped graphene segment. (b) AFM line profile of the folded graphene along the blue dashed line shown in (a); the inset shows a zoom-in view of the folding edge with a "hump" height. (c) AFM line profile of the flat non-folded graphene segment along the red dashed line shown in (a).

and its measured height may be attributed to a few factors, such as the surface roughness of the substrate, the free amplitude of the AFM cantilever, and the change in the tip-sample interaction when the AFM tip scans over the sample surface.[21] Therefore, the measured graphene height on the substrate does not inform directly its actual thickness and number of layers. However, the step height in the folded graphene region can be considered as a more reliable value of the graphene thickness.[22] The measured upper step height of 1.07 nm is close to the theoretical thickness value 1.02 nm of a trilayer graphene sheet. Therefore, it is concluded that the partially folded sheet shown in Figure 1(a) is a trilayer graphene. The analysis also indicates that a gap of about 0.5 nm exists between the bottom surface of the graphene and the supporting substrate.

It is of importance to point out that the surface roughnesses of both the graphene and the supporting substrate are important factors in the graphene thickness measurement. The roughness of the graphene sheet is measured to be 1.35 Å based on the calculated root-mean-square (rms) value of its scanning profile, while the roughness of the substrate is measured to be 1.49 Å. The results show that the graphene is slightly smoother than the SiO_2 substrate, indicating that the graphene sheet conforms closely to the underlying SiO_2 substrate.[23,24] The intrinsic ripple effect in graphene due to its thermal instability also has an influence on its surface roughness. However, the ripple effect is more prominent in monolayer graphene due to its ultra-low bending rigidity, and in free-standing graphene due to the fact that the substrate reportedly suppresses the ripple effect in supported graphene sheets.[23–25] Our measurement data are consistent with the previously reported findings that the corrugation properties of graphene are mainly contributed by the roughness of the underlying substrate.[26,27] The thickness of the folded graphene shown in Figure 1 and its rms value is calculated to be 1.07 ± 0.19 nm by taking into account its surface roughness in the flat adhered region. It is noted that the thickness range is higher than the thickness of bilayer graphene (0.68 nm), while smaller than that of quadrilayer graphene (1.36 nm). Therefore, the conclusion of a trilayer graphene for the tested sample shown in Figure 1 remains valid with the consideration of the graphene surface roughness.

The height of the folding edge (i.e., the hump shown in the inset of Figure 1(b)) and its rms value is measured to be 5.7 ± 1.35 Å with respect to the top surface of the folded graphene segment. The folding conformation of graphene on a flat substrate depends on a few factors such as its folding length, thickness, bending rigidity, adhesion with the substrate as well as the adhesion in the flat adhered region. For graphene with multiple layers, its bending rigidity is dependent not only on its thickness, but also on the interlayer interactions. If we consider a trilayer graphene as a laminated structure that is composed of three identical sheets, its bending rigidity, based on classical continuum mechanics theory, can vary from 3 times that of individual sheets if all the neighboring sheets can slide freely with respect to each other, to 27 times if all the sheets are perfectly bonded and no interlayer sliding is allowed. Below we interpret the experimental measurements on self-folding of trilayer graphene using a nonlinear CM model based on beam theory and MD simulations.

B. Continuum mechanics modeling

Figure 2(a) shows the schematic diagram of a self-folded graphene sheet on a flat substrate. The red curve represents the middle-plane of the folded graphene, which consists of a curved region of a length L and a flat region of a length L_0. The total length of the folded graphene is $L_{tot} = L + L_0$. The graphene adheres within the flat region due to van der Waals (vdW) interactions. The equilibrium distance between the parallel, adhered region of the folded graphene is denoted as d. The curved region is formed due to the resistance to bending of the graphene, and is divided into four segments by five points, A, B, C, D, and E, as shown in Figure 2(a). Points A, C, D, and E represent the respective boundaries in the deformation curve, while point B is the inflection point that is of zero curvature. The equilibrium equations of the folded sheet are given as[8]

$$\frac{dM}{ds} + V = 0, \frac{dV}{ds} + N\frac{d\theta}{ds} = 0, \frac{dN}{ds} - V\frac{d\theta}{ds} = 0, \quad (1)$$

where θ is the rotation angle; s is the arc length measured from point A; M, V, and N are the bending moment, shear force, and normal force within the sheet, respectively. It is noted that $M = \lambda \cdot \kappa = \lambda(d\theta/ds)$, in which λ is the bending

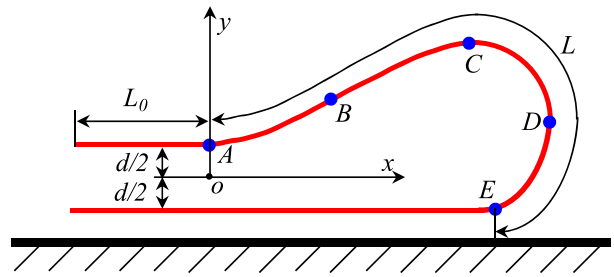

(a)

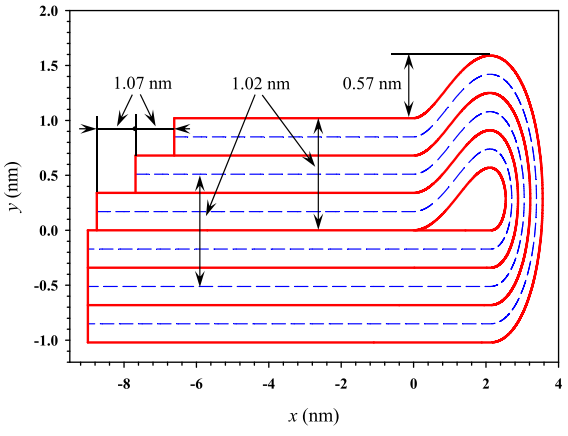

(b)

FIG. 2. (a) Schematic illustation of a self-folded graphene on a flat substrate. (b) The predicted folding profile of a trilayer graphene with a bending stiffness of 6.57 eV using the continuum mechanics model given by Eq. (1). The total length of the folded graphene $L_{tot} = 13.0$ nm. The dashed line represents the middle-plane of each graphene layer.

stiffness per unit length of the graphene sheet and $\kappa = d\theta/ds$ is its bending curvature. Positions A ($y = d/2$, $\theta = 0$) and E ($y = -d/2$, $\theta = -\pi$) are two delamination fronts, and their respective bending curvatures are given as $\kappa_A = (2\Gamma_g/\lambda)^{1/2}$ at position A and $\kappa_E = (2\Gamma_s/\lambda)^{1/2}$ at position E,[28,29] in which Γ_g is the adhesion energy per unit area in the flat adhered region, and Γ_s is the adhesion energy per unit area between the graphene sheet and the substrate. The exact bending curvature of the folded sheet can be obtained through solving Eq. (1) with the aforementioned boundary conditions. It is noted that Eq. (1) can only provide solutions of equilibrium in self-folding of graphene, while its stability will be determined through an energy analysis.

The graphene folding configuration is largely determined by the competition between the adhesion over the flat adhered region and the bending over the curved region. The adhesion interaction tends to fold the graphene sheet, while the bending energy provides resistance against folding. We define the flat graphene as the ground energy state, and the total energy of the folded graphene is calculated as $U_{tot} = U_{bend} - \Delta E$, where U_{bend} is the bending energy stored in the curved portion and ΔE is the adhesion energy in the flat adhered region. A stable folding state occurs when the adhesion energy ΔE exceeds the required bending deformation energy U_{bend}; that is, $U_{tot} < 0$. For a short graphene, the adhesion energy may be too small to balance the bending energy (i.e., $U_{tot} > 0$). Therefore, the equilibrium self-folding states of graphene are energetically unstable. A long graphene leads to $U_{tot} < 0$, and the equilibrium self-folding states become energetically stable. Therefore, there exists a critical threshold length of the graphene sheet L_c, above which the folding configuration is stable. For $L_{tot} < L_c$, the graphene sheet is stable only when it stays in a flat configuration. Similar approaches have been employed in the investigation of suspended self-folded carbon nanotubes[30] and graphene.[8,16] The bending energy in the folded sheet is given by $U_{bend} = \int_0^L \frac{j}{2}\kappa^2 ds$, while $\Delta E = \Gamma_g L_0$ reflects the adhesion energy of the flat adhered region. The critical threshold graphene length for a stable folding state can be derived from $U_{bend} = \Delta E$.

We analyze the folded graphene shown in Figure 1(a) using the above-mentioned CM model. The equilibrium distance between two parallel trilayer graphene $d = 1.02$ nm is employed in the CM modeling. The adhesion energy between trilayer graphene and SiO_2 substrates is reported to be within 0.275–0.4 J/m^2 in the literature,[31] and the middle value of the reported range $\Gamma_s = 0.338$ J/m^2 is adopted in the analysis. The adhesion energy between two parallel monolayer graphene is reported to be 1.45 eV/nm^2 or 0.232 J/m^2.[32,33] It is noted that the vdW interactions between non-contacting graphene layers also contribute to the adhesion interaction, and follow a power function of the interlayer distance with an exponent of -4.[34] For trilayer graphene, Γ_g is calculated to be 0.267 J/m^2. The bending stiffness of the folded graphene sheet can be obtained through fitting the predicted hump height to the measured value. The critical threshold length for a stable self-folding configuration of trilayer graphene on SiO_2 substrates is obtained as $L_c = 13.0$ nm with a length of the curved region $L = 4.96$ nm. Figure 2(b) shows the predicted deformational profile of a self-folded trilayer graphene with a total length $L_{tot} = L_c$ by using the above-mentioned theoretical model with a fitting bending stiffness of 6.57 eV. The middle-plane of the folded graphene has a bending curvature of 0.71/nm at point A and 0.80/nm at point E. The bending stiffness of the trilayer graphene is found to be within the range of 5.9–7.4 eV by taking into acount the measurement error in the graphne folding hump.

Figure 3 shows the dependence of the total system energy U_{tot} on the total length L_{tot} for a self-folded trilayer graphene. The plot can be divided into three regimes that correspond to different self-folding states of trilayer graphene. For the total length $L_{tot} < 4.96$ nm, there is no equlibrium solution for Eq. (1). Therefore, the graphene with a length shorter than 4.96 nm cannot be self-folded and stay in equilibrium. The graphene can only stay in an equilibrium and stable state in flat configurations. For $4.96\,\text{nm} < L_{tot} < 13\,\text{nm}$ (red line region), the unique self-folding configuration can be obtained. However, the bending energy exceeds the ahesion energy, i.e., $U_{tot} > 0$. The equilibrium self-folding state is energetically unstable. For $L_{tot} > 13.0$ nm (blue line region), the system energy U_{tot} is less than zero and the equilibrium self-folding state is energetically stable. It is noted that *ab initio* predictions of the bending stiffness of monolayer graphene is reported to be within 1.4–1.6 eV.[35,36] Therefore, the bending stiffness of trilayer graphene obtained from our experimental measurements is approximately four times the values reported for monolayer graphene. Our results about the bending stiffness of trilayer graphene suggest that relatively free interlayer sliding occurs in the trilayer graphene during its folding process, which can be ascribed to the weak interlayer vdW interaction in graphene. Our observation is consistent with a prior report that a graphene sheet can move relatively freely on top of another graphene sheet on a flat substrate.[37] The results of the relatively low bending rigidity also indicate that there is no constraint to the free ends of the folded graphene segment, and relative slides shall occur between the free ends of

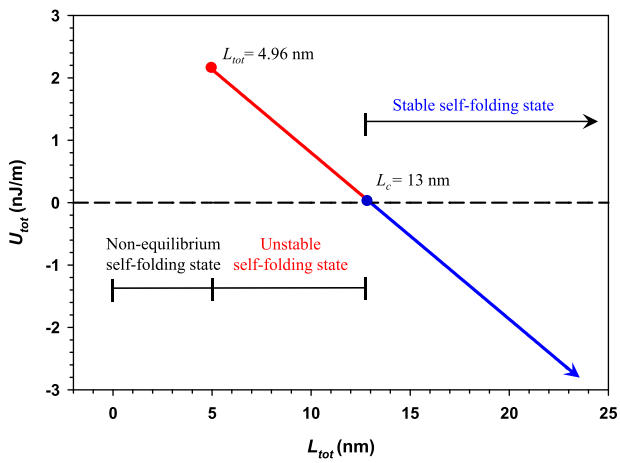

FIG. 3. The dependence of the total system energy U_{tot} of a self-folded trilayer graphene on a flat SiO_2 substrate on the total length of the folded graphene L_{tot}. The plot is divided into three regimes corresponding to different graphene self-folding states. The red dot indicates the smallest length of graphene that can stay in an equilibrium self-folding state. The blue dot indicates the critical total length of graphene that can stay in an equilibrium and energetically stable self-folding state. The blue curve represents the equilibrium and energetically stable self-folding state of graphene.

neighboring layers. Assuming that the bending rigidity of graphene sheets is linearly appropriate to its number of layers, our analysis yields a value of 2.19±0.2 eV as the bending stiffness of monolayer graphene. Prior studies on the bending stiffness of graphene with fixed-fixed ends using electrostatic bending techniques report values of 7.1 eV for monolayer graphene and 126 eV for trilayer graphene.[15] It is likely that these reported values are greatly enhanced by the stretching effect in graphene. By assuming that all the graphene layers have the same and intact length during the folding process, the deformation profiles of each layer in the folded trilayer graphene are calculated and displayed in Figure 2(b). Our results show that there is a horizontal slide of about 1.07 nm between the free ends of the neighboring graphene layers.

C. Molecular dynamics simulations

We perform MD simulations to gain more insights into graphene folding at an atomistic level. In the MD simulation, we adopt the adaptive intermolecular reactive empirical bond order (AIREBO) potential.[38] It should be noted that this potential is best suited for systems containing only hydrogen and carbon atoms,[8,39,40] which makes it accessible for all-carbon systems. *12–6* Lennard-Jones potential is adopted to describe the vdW interactions based on the Lorentz-Berhelot mixing rule. To terminate the unphysical high bond force arising from improper cut-off functions, we set the cut-off distance as 8 Å. Periodic boundary conditions are also applied in the simulation. The conjugate gradient algorithm is employed to perform the energy minimization until the ratio between the total energy change between two successive iterations and the energy magnitude is less than or equal to 10^{-8}. NVT (the abbreviations of particles (N), system volume (V), and temperature (T)) ensemble simulations with a constant temperature 300 K are carried out based on the Berendsen thermostat.[41]

Figure 4(a) shows the self-folded conformation of a trilayer graphene sheet with a dimension of 30 nm × 21 nm on a silicon substrate of 1.02 nm in thickness. All graphene layers are set up in zigzag orientations. The left end of the graphene sheet that is marked in red is fixed, while the other end marked in blue is tethered to fold the graphene. The tethered end first moves vertically along the y-axis until reaching a height of 2.85 nm with a velocity of 0.03 nm per 0.05 ps (i.e., 0.6 nm/ps), and then travels a horizontal distance of 27.5 nm with the same velocity along the negative x-axis. The system is relaxed in a short time period of 0.05ps after each step in the tethered end moves to make sure that the mechanical folding process reaches a steady state. After the mechanical folding process is completed, the whole system is relaxed for quite a long time (about 100 ps) and undergoes a self-folding and adjusting process. Figure 4(b) depicts the height profile of each layer in the folded trilayer graphene on the silicon substrate. The height of the folding edge is found to be about 9.6 Å. Figure 4(b) also shows the predicted folding profiles (black curves) using the CM model given by Eq. (1) with a fitting bending stiffness of 7.4 eV, which displays an excellent agreement with the MD simulation results for all three layers. It is noted that a value of 0.151 J/m^2 is

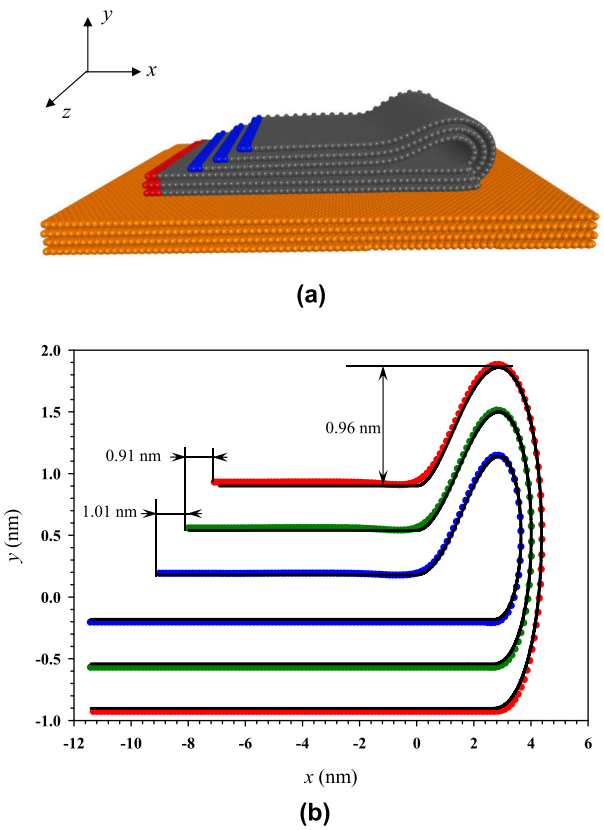

FIG. 4. (a) The predicted conformation of a self-folded trilayer graphene on a silicon substrate using MD simulations. (b) Deformation profile of each graphene layer (middle-plane) in a folded trilayer graphene on the substrate. The dots represent the MD results, while the solid curves represent the results obtained using the continuum mechanics model given by Eq. (1).

employed as the adhesion energy between graphene sheets and silicon substrates in the MD simulations.[42] The bending stiffness of trilayer graphene from MD simulations (7.4 eV) is consistent with the value obtained based on the experimental measurements (5.9–7.4 eV). It is noted that the ripple effect in graphene is size-dependent[43] and is not prominent in our MD results due to the small graphene size employed in the simulations. The values of the relative interlayer slides at the free graphene ends are also obtained. MD simulations predict that the free-end of the outer-layer graphene slides about 0.91 nm with respect to that of the middle-layer graphene, while a slide distance of 1.01 nm between the middle- and the inner-layer graphene sheets. Both values are close to the CM results, which are found to be 1.07 nm for both the two interlayer slides. The good agreements between the CM modeling and the MD simulation results clearly demonstrate that the self-folding behavior of graphene can be well described using the nonlinear CM model.

III. CONCLUSION

In summary, we investigate the local self-folding behavior of graphene on flat substrates by using AFM in conjunction with nonlinear CM modeling and MD simulations. Our study reveals that the bending stiffness of trilayer graphene is about four times the reported values for monolayer graphene. The analysis suggests an intriguing free sliding

phenomenon occurs between two neighboring graphene layers in the global graphene folding process. The study demonstrates that it is a plausible venue to qualify the pure bending stiffness of graphene through measuring its self-folding conformation on flat substrates. This work is useful in better understanding the structural and mechanical properties of graphene and in the pursuit of its applications, in particular, as programmable nanoscale origami structures.

ACKNOWLEDGMENTS

This work was partially supported by US Air Force Office of Scientific Research under the Grant No. FA9550-11-1-0042.

[1]C. Lee, X. Wei, J. W. Kysar, and J. Hone, Science **321**, 385 (2008).
[2]K. S. Novoselov, A. K. Geim, S. V. Morozov, D. Jiang, Y. Zhang, S. V. Dubonos, I. V. Grigorieva, and A. A. Firsov, Science **306**, 666 (2004).
[3]X. Li, X. Wang, L. Zhang, S. Lee, and H. Dai, Science **319**, 1229 (2008).
[4]J. S. Bunch, A. M. van der Zande, S. S. Verbridge, I. W. Frank, D. M. Tanenbaum, J. M. Parpia, H. G. Craighead, and P. L. McEuen, Science **315**, 490 (2007).
[5]S. Stankovich, D. A. Dikin, G. H. B. Dommett, K. M. Kohlhaas, E. J. Zimney, E. A. Stach, R. D. Piner, S. T. Nguyen, and R. S. Ruoff, Nature **442**, 282 (2006).
[6]H. C. Schniepp, K. N. Kudin, J.-L. Li, R. K. Prud'homme, R. Car, D. A. Saville, and I. A. Aksay, ACS Nano **2**, 2577 (2008).
[7]J. Zhang, J. Xiao, X. Meng, C. Monroe, Y. Huang, and J.-M. Zuo, Phys. Rev. Lett. **104**, 166805 (2010).
[8]X. Meng, M. Li, Z. Kang, X. Zhang, and J. Xiao, J. Phys. Appl. Phys. **46**, 055308 (2013).
[9]S. Zhu and T. Li, ACS Nano **8**, 2864 (2014).
[10]W. Zhu, T. Low, V. Perebeinos, A. A. Bol, Y. Zhu, H. Yan, J. Tersoff, and P. Avouris, Nano Lett. **12**, 3431 (2012).
[11]K. Kim, Z. Lee, B. D. Malone, K. T. Chan, B. Alemán, W. Regan, W. Gannett, M. F. Crommie, M. L. Cohen, and A. Zettl, Phys. Rev. B **83**, 245433 (2011).
[12]M. Becton, L. Zhang, and X. Wang, Chem. Phys. Lett. **584**, 135 (2013).
[13]L. Zhang, X. Zeng, and X. Wang, Sci. Rep. **3**, 3162 (2013).
[14]V. B. Shenoy and D. H. Gracias, MRS Bull. **37**, 847 (2012).
[15]N. Lindahl, D. Midtvedt, J. Svensson, O. A. Nerushev, N. Lindvall, A. Isacsson, and E. E. B. Campbell, Nano Lett. **12**, 3526 (2012).
[16]S. Cranford, D. Sen, and M. J. Buehler, Appl. Phys. Lett. **95**, 123121 (2009).
[17]K. Kim, V. I. Artyukhov, W. Regan, Y. Liu, M. F. Crommie, B. I. Yakobson, and A. Zettl, Nano Lett. **12**, 293 (2012).
[18]D. Graf, F. Molitor, K. Ensslin, C. Stampfer, A. Jungen, C. Hierold, and L. Wirtz, Nano Lett. **7**, 238 (2007).
[19]A. Gupta, G. Chen, P. Joshi, S. Tadigadapa, and P.C. Eklund, Nano Lett. **6**, 2667 (2006).
[20]C. Casiraghi, A. Hartschuh, E. Lidorikis, H. Qian, H. Harutyunyan, T. Gokus, K. S. Novoselov, and A. C. Ferrari, Nano Lett. **7**, 2711 (2007).
[21]P. Nemes-Incze, Z. Osváth, K. Kamarás, and L. P. Biró, Carbon **46**, 1435 (2008).
[22]K. S. Novoselov, D. Jiang, F. Schedin, T. J. Booth, V. V. Khotkevich, S. V. Morozov, and A. K. Geim, Proc. Natl. Acad. Sci. USA **102**, 10451 (2005).
[23]C. H. Lui, L. Liu, K. F. Mak, G. W. Flynn, and T. F. Heinz, Nature **462**, 339 (2009).
[24]W. G. Cullen, M. Yamamoto, K. M. Burson, J. H. Chen, C. Jang, L. Li, M. S. Fuhrer, and E. D. Williams, Phys. Rev. Lett. **105**, 215504 (2010).
[25]T. Li and Z. Zhang, J. Phys. Appl. Phys. **43**, 075303 (2010).
[26]E. Stolyarova, K. T. Rim, S. Ryu, J. Maultzsch, P. Kim, L. E. Brus, T. F. Heinz, M. S. Hybertsen, and G. W. Flynn, Proc. Natl. Acad. Sci. USA **104**, 9209 (2007).
[27]M. Ishigami, J. H. Chen, W. G. Cullen, M. S. Fuhrer, and E. D. Williams, Nano Lett. **7**, 1643 (2007).
[28]M. Zheng and C. Ke, Small **6**, 1647 (2010).
[29]Y. Zhao, X. Chen, C. Park, C. C. Fay, S. Stupkiewicz, and C. Ke, J. Appl. Phys. **115**, 164305 (2014).
[30]W. Zhou, Y. Huang, B. Liu, K. C. Hwang, J. M. Zuo, M. J. Buehler, and H. Gao, Appl. Phys. Lett. **90**, 073107 (2007).
[31]S. P. Koenig, N. G. Boddeti, M. L. Dunn, and J. S. Bunch, Nat. Nanotechnol. **6**, 543 (2011).
[32]J. Xiao, B. Liu, Y. Huang, J. Zuo, K.-C. Hwang, and M.-F. Yu, Nanotechnology **18**, 395703 (2007).
[33]F. Ortmann, F. Bechstedt, and W. G. Schmidt, Phys. Rev. B **73**, 205101 (2006).
[34]J. Sarabadani, A. Naji, R. Asgari, and R. Podgornik, Phys. Rev. B **84**, 155407 (2011).
[35]D.-B. Zhang, E. Akatyeva, and T. Dumitrică, Phys. Rev. Lett. **106**, 255503 (2011).
[36]N. G. Chopra, L. X. Benedict, V. H. Crespi, M. L. Cohen, S. G. Louie, and A. Zettl, Nature **377**, 135 (1995).
[37]X. Feng, S. Kwon, J. Y. Park, and M. Salmeron, ACS Nano **7**, 1718 (2013).
[38]S. J. Stuart, A. B. Tutein, and J. A. Harrison, J. Chem. Phys. **112**, 6472 (2000).
[39]V. B. Shenoy, C. D. Reddy, and Y.-W. Zhang, ACS Nano **4**, 4840 (2010).
[40]Y. Zheng, N. Wei, Z. Fan, L. Xu, and Z. Huang, Nanotechnology **22**, 405701 (2011).
[41]H. J. C. Berendsen, J. P. M. Postma, W. F. van Gunsteren, A. DiNola, and J. R. Haak, J. Chem. Phys. **81**, 3684 (1984).
[42]Z. Zong, C.-L. Chen, M. R. Dokmeci, and K. Wan, J. Appl. Phys. **107**, 026104 (2010).
[43]A. K. Singh and R. G. Hennig, Phys. Rev. B **87**, 094112 (2013).